LIMNOLOGY AND OCEANOGRAPHY
Letters

ASLO
Open Access

Limnology and Oceanography Letters 2019

doi: 10.1002/lol2.10133

LETTER

Capacity of the common Arctic picoeukaryote *Micromonas* to adapt to a warming ocean

Ina Benner,[1] *Andrew J. Irwin*[2a] *Zoe V. Finkel*[1b]*

[1]Environmental Science Program, Mount Allison University, Sackville, New Brunswick, Canada; [2]Department of Mathematics and Computer Science, Mount Allison University, Sackville, New Brunswick, Canada

Scientific Significance Statement

Polar regions are experiencing the most rapid temperature increases due to climate change with anticipated far-reaching effects on marine primary production and the carbon cycle. Based on short-term experiments, it has been hypothesized that Arctic *Micromonas*, a dominant member of the phytoplankton community, would eventually be inhibited by the increased temperatures associated with climate warming. Our experiments show that *Micromonas polaris* has the capacity to change its thermal performance curve, optimum temperature for growth, and growth rate in only a few hundred generations or two years, which should alter how we model anticipated changes in phytoplankton community structure in polar waters over the coming century.

Abstract

Phytoplankton are sensitive to temperature and other environmental conditions expected to change with warming over the next century. We quantified the capacity of an ecologically dominant Arctic phytoplankton species, *Micromonas polaris*, to adapt to changes in temperature, increased temperature and irradiance, and increased temperature and periodic nitrogen starvation, over several hundred generations. When originally isolated, this strain of *Micromonas* had its maximum growth rate at 6°C, and its growth rate declined above 10°C. We find an evolutionary increase in growth rate, with the largest increases associated with the elevated temperature treatments, especially when combined with repeated nitrate starvation. After several hundred generations of exposure, the growth rate of *Micromonas* under 13°C almost doubled and was higher than under 6°C. This increase in growth rate is consistent with the Arrhenius model of temperature effects on metabolism and suggests a general hypothesis for the evolutionary potential of phytoplankton to respond evolutionarily to temperature change.

*Correspondence: zfinkel@dal.ca

[a]Present address: Department of Mathematics and Statistics, Dalhousie University, Halifax, Nova Scotia, Canada

[b]Present address: Department of Oceanography, Dalhousie University, Halifax, Nova Scotia, Canada

Author Contribution Statement: I.B. and Z.V.F. designed the study. I.B. performed the experiments. I.B., A.J.I., and Z.V.F. performed analyses and wrote the paper.

Data Availability Statement: Data and metadata are available in the figshare.com data repository at https://dx.doi.org/10.6084/m9.figshare.4264499 (doi 10.6084/m9.figshare.4264499).

Associate editor: Jeffrey Krause

Additional Supporting Information may be found in the online version of this article.

The Arctic is undergoing rapid environmental change. Arctic warming is causing a reduction in the annual temporal duration and spatial extent of sea ice, increases in light availability in the sea surface, and the potential annual growing season for phytoplankton (Osborne et al. 2018). Changes in net primary production (NPP) by phytoplankton and sea ice algae are expected to have widespread impacts on the Arctic food web and the global carbon cycle. Arrigo and Van Dijken (2011) have extrapolated that the complete loss of Arctic sea ice could increase annual Arctic NPP to ~ 730 Tg C a^{-1} relative to an estimated average rate of 438 Tg C a^{-1} from 1978 to 1998. There is significant spatial and temporal variability in Arctic marine NPP (Tremblay et al. 2015) and much uncertainty in projections for how future warming will alter NPP in the Arctic Ocean (Vancoppenolle et al. 2013). Increasing cloudiness (Bélanger et al. 2013) and decreases in nitrate availability in the sea surface may moderate and even cause decreases in NPP (Capotondi et al. 2012; Vancoppenolle et al. 2013). In the contemporary Arctic ocean, phytoplankton achieve their optimal growth rate at about 6.5°C and there is speculation that a warming ocean may restructure phytoplankton communities once temperatures exceed the ideal range of temperatures (Coella-Camba and Agusti 2017).

Climate-driven changes in phytoplankton production and community composition are expected to influence trophic transfer of phytoplankton carbon to the upper food web and export to the deep sea. Phytoplankton communities dominated by small cells will often have lower trophic efficiency and rates of carbon export to the deep sea than communities dominated by larger cells (Laws et al. 2000; Finkel et al. 2010). Historically, large diatoms have dominated communities in the more eutrophic regions of the Arctic, such as Baffin Bay and Lancaster Sound, while small flagellate-dominated communities are found in the oligotrophic regions of the eastern Beaufort Sea, peripheral Amundsen Gulf, and the central region of the Canadian Arctic Archipelago (Ardyna et al. 2017). Recent increases in sea ice melt and increased stratification of the waters in the Canadian Arctic Basin have been associated with an increase in the abundance of small flagellates such as *Micromonas* (Li et al. 2009).

Micromonas is a common and often dominant member of phytoplankton communities in the Arctic (Not et al. 2005; Lovejoy et al. 2007; Balzano et al. 2012; Simon et al. 2017). Field data and short-term acclimation experiments indicate that both warming and ocean acidification may increase the growth rate and ecological role of *Micromonas* in the Arctic (Lovejoy et al. 2007; Li et al. 2009; Hoppe et al. 2018). There is evidence that phytoplankton may have the capacity to evolve, altering their responses to changing conditions (e.g., Schaum et al. 2016; Walworth et al. 2016). More information on both the acclimation and adaptation potential of key Arctic phytoplankton species, such as *Micromonas*, in response to the environmental changes expected with climate warming is required to improve our understanding of how phytoplankton community structure may change in a warming Arctic.

Our objective was to determine if the geographically widespread Arctic picoprasinophyte *Micromonas* has the evolutionary capacity to alter its growth rate in response to environmental conditions expected to change with future warming and water column stratification. We addressed this through long-duration laboratory experiments on *M. polaris*, quantifying its growth rate over hundreds of generations of exposure to increased temperature, increased temperature and irradiance, and an increase in temperature in conjunction with periodic nitrate stress. We find evidence of evolutionary increases in growth rate under several of the treatments.

Material and methods

Arctic *Micromonas* strain CCMP 2099, now identified as *M. polaris* (Simon et al. 2017), was obtained from the Provasoli-Guillard National Center for Marine Algae and Microbiota. Cultures were grown in natural seawater from Cape Tormentine, Canada (salinity 30–33) enriched with f/2 trace metals and vitamins, as well as 7.5 nmol L^{-1} sodium selenite. Nitrate and phosphate additions were reduced from the original f/2 concentrations to 120.1 μmol L^{-1} and 12.4 μmol L^{-1}, respectively, to moderate the maximum cell density of lines allowed to grow into stationary phase as described in the following paragraph. The medium was filter-sterilized (Pall Acropak 0.8/0.2 μm capsule filter). Experimental lines were initiated from small innocula; cultures initiated from single cells were not viable. Six replicate lines were maintained per treatment. Axenic technique was applied but the cultures were not free of bacteria.

Five treatments were investigated. Three temperature treatments: 2°C, 6°C, or 13°C at 100 μmol photons m^{-2} s^{-1} (identified as 2C, 6C, and 13C treatments). In addition, a 13°C treatment was grown at elevated irradiance of 220 μmol photons m^{-2} s^{-1} (13HL treatment). These four treatments were maintained as semicontinuous diluted batch cultures. All cultures were transferred into new media in the exponential growth phase at a cell density of 6.0–8.0 × 10^6 cells mL^{-1} and diluted down to 1.0 × 10^6 cells mL^{-1}. A fifth treatment was grown at 13°C and run repeatedly into stationary phase nitrate limitation (13LN treatment); cultures were transferred into new media the second day in the stationary phase (as determined at the initiation of the experiment) at a cell density between 12.0–16.0 × 10^6 cells mL^{-1} and diluted down to ~ 1.65 × 10^6 cells mL^{-1}. All treatments were grown under a 12:12 light:dark cycle.

Cell density was counted using a light microscope (Zeiss, Axio Imager 2, 40X objective) and hemocytometer or with a flow cytometer (BD, Accuri™ C6 Plus). Growth rates were

calculated using the cell density at the beginning (n_0) and end of each transfer (n) using the following equation:

$$\mu = \frac{\ln(n) - \ln(n_0)}{t} \quad (1)$$

where t was the time between transfers in days. For the periodically nitrate-limited treatment, the culture spent approximately 2 d in stationary phase and 2 d in lag phase between each serial dilution at time 0. Using the full time period to calculate growth rate would provide an estimate of growth rate considerably smaller than the growth rate during exponential phase in this treatment and make comparisons with the 13°C nitrate-replete cultures more difficult. For this reason, we approximated the exponential growth rate in the periodically nitrate-limited treatment as

$$\mu = \frac{\ln(n) - \ln(n_0)}{t - 4}. \quad (2)$$

This calculation assumes there is no change in the duration of the lag and stationary phases, but they may have changed throughout the experiment.

Fitness tests were conducted on the 13°C treatment. Three of the six lines of the 13°C treatment were subcultured and transferred to 2°C and 6°C. The lines for the fitness test were chosen with the lowest, highest, and average growth rate of the six lines. After an acclimation period of 8–10 generations, growth rates were determined. The experiment was terminated after approximately 260, 270, 330, 340, and 170 generations for the 2C, 6C 13C, 13HL, and 13LN treatments, respectively.

Since growth rates were estimated at each transfer from a two-point estimate, the uncertainty in each growth rate estimate led to substantial variability over short periods of time; therefore, we focus on the long-term trend rather than this short-term variability. Changes in growth rate (μ, d^{-1}) over the evolutionary experiment were analyzed by regression with a linear model ($\mu = \mu_0 + mt$) and a nonlinear model using a Michaelis–Menten saturating function ($\mu = \mu_0 + \frac{\mu_D t}{t+K}$) where t is the time in generations since the start of the experiment for each treatment, μ_0 is the growth rate at time 0, μ_D is the projected increase in growth rate at the end of the evolutionary trajectory, and K is the number of generations required to achieve half of this change (similar to Barrick et al. 2009). We use time measured in generations rather than days as we are seeking to identify evolutionary changes and wish to be able to compare the evolutionary rates under contrasting conditions with very different growth rates (d^{-1}). Outliers were identified with the R package robustbase (Maechler et al. 2018) and removed if the robustness weight for a point as determined by the function lmrob was less than 0.3. Models were fit with separate parameters for each bottle within each treatment and for a single set of parameters for all bottles pooled within a treatment. Parameters were estimated with a Bayesian approach using the R packages brms and rstan (Bürkner 2018; Carpenter et al. 2017). The leave-one-out information criterion (LOOIC) was used to identify the model with the best tradeoff between parsimony and fit to the data.

Results

Growth rates increased throughout the evolution experiment in all lines and treatments, although the trend varied over time and across treatments (Table 1; Fig. 1). The growth rate increase was lowest (μ_D) and slowest (K) in the 2°C treatment. The 6°C treatment showed the next smallest increase in growth rate over the course of the experiment. The 13°C, 13°C HL, and 13°C LN treatments had the largest increases in growth rate by the end of the experiment. With the exception of the 13°C LN treatment, all of the treatments exhibited a saturating increase in growth rate with increasing number of generations of exposure (Fig. 1; Table 1). The 2°C treatment exhibited very little change in growth rate over 260 generations of exposure, and thus little evidence of saturation, while the 13°C LN treatment exhibited a nearly linear increase in growth rate throughout the 170 generations of the experiment (Figs. 1, 2). For the 13°C LN treatment, the growth rate corresponds to a realized average growth rate between dilutions and may not correspond to the maximum exponential growth rate. This growth rate may not directly correspond to changes in exponential growth rate if there was a change in lag or stationary phase duration or in resource use efficiency, which was not monitored. In all cases, the models fit to each line/bottle separately were deemed inferior (had larger LOOIC scores) than the models fit to pooled data within treatments; pooled parameter estimates are provided in Table 1. The fitness test on cultures grown from the 13°C treatment at 250 generations found no significant change in growth rate at 2°C, an 8% decrease in growth rate at 6°C, and a small (3%) increase in 13HL, relative to the growth rate of lines evolved in the corresponding treatments (i.e., the 2C, 6C, and 13HL treatments). This indicates that there was a shift in the optimal growth temperature from 6°C to 13°C over the course of the experiment in the 13°C treatment.

Discussion

M. polaris CCMP 2099 is a common and ecologically important member of Arctic phytoplankton communities (Not et al. 2005; Lovejoy et al. 2007; Balzano et al. 2012; Simon et al. 2017). Traditional shorter-term physiological experiments have shown that the growth rate of *M. polaris* is optimal between 6°C and 8°C, inhibited above 10°C and that it is unable to tolerate temperatures above 12.5°C (Lovejoy et al. 2007). These results have been used to hypothesize that *M. polaris* may decline in abundance and geographic extent with significant warming in the Arctic. Demory et al. (2019) have hypothesized that *Micromonas* may evolve in response to

Table 1. Parameters describing how exponential growth rate, μ, increases with the number of generations, t, since the start of the evolutionary experiment for each treatment.

Treatment	μ_0 (d^{-1})	μ_D (d^{-1})	K (gen)	n	n_{out}
2°C	0.28 (0.27, 0.29)	0.072 (0.043, 0.11)	210 (58, 380)	321	0
6°C	0.36 (0.33, 0.38)	0.18 (0.14, 0.24)	160 (57, 310)	274	2
13°C	0.28 (0.26, 0.30)	0.29 (0.26, 0.33)	120 (77, 200)	414	15
13°C HL	0.35 (0.33, 0.37)	0.26 (0.22, 0.31)	170 (96, 270)	421	8
13°C LN	0.22 (0.20, 0.24)	0.46 (0.37, 0.58)	190 (120, 280)	203	10
	μ_0 (d^{-1})	m (d^{-1} 1000 gen^{-1})			
13°C LN	0.24 (0.22, 0.25)	1.37 (1.22, 1.53)			

Data for each treatment is fit to the saturating function model $\mu = \mu_0 + \mu_D t/(t + K)$, where μ_0 is the exponential growth rate at $t = 0$, μ_D is the projected maximum increase in exponential growth rate at the end of the evolutionary trajectory, and K is the time, in generations, for half of this increase to be achieved. The table lists the posterior mean of each parameter and the 95% credible interval from model fits using brms (Bürkner 2018). Parameters for a linear model, $\mu = \mu_0 + m(t/1000)$, are also reported for the 13°C LN treatment. The leave-one-out cross-validation information criterion favored the saturating function for all treatments except for the 13°C LN treatment which favored the linear model. Sample size, n, is the number of two-point growth rate estimates used for each model fit. A small number, n_{out}, of growth rates were deemed to be outliers and removed (using the R package robustbase; Maechler et al. 2018).

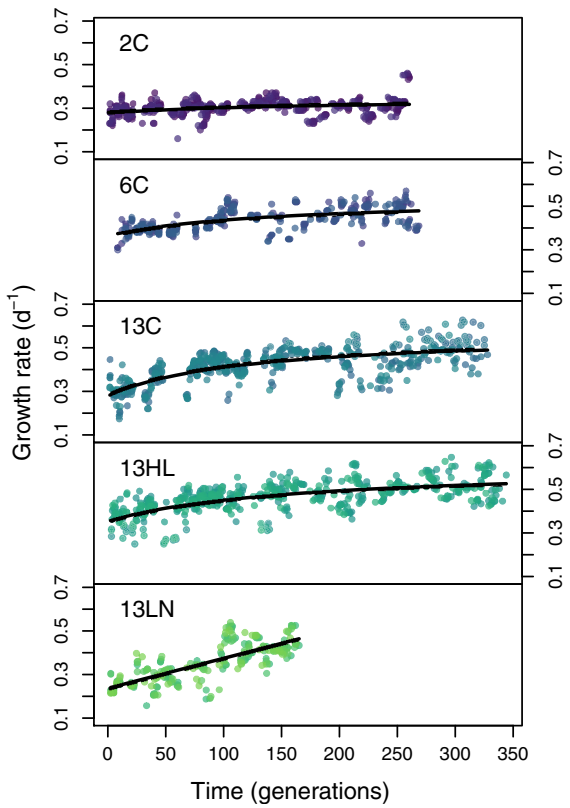

Fig. 1. Exponential growth rates (d^{-1}) measured throughout the evolution experiment estimated from successive pairs of cell counts. Individual bottles ($n = 6$) within treatments are distinguished by color shades. Treatment legend: 2°C (2C), 6°C (6C), 13°C (13C), 13°C and high irradiance (13HL), and 13°C and periodic nitrate limitation (13LN). The nonlinear model fit (Table 1) is shown as a solid line.

temperature change over the next century. Our long-term study demonstrates that populations of *M. polaris* have the capacity to adapt to higher temperature (13°C), higher temperature and irradiance (13°C and 200 μmol m^{-2} s^{-1}), and higher temperature with periodic nitrate depletion within 200 generations (Figs. 1, 2; Table 1). Padfield et al. (2016) found the freshwater alga, *Chlorella vulgaris* was able to evolve tolerance to high temperature after approximately 100 generations. These results, in conjunction with related studies on other key phytoplankton species, suggest that evolutionary dynamics will likely play a significant role in shaping the response of phytoplankton communities to climate change over the next centuries (Bell and Collins 2008).

Here, we observe rapid increases in fitness in all our treatments (within 100–200 generations), with close replication across lines (Table 1; Fig. 2). Fitness increases within hundreds of generations have been reported in several studies on eukaryotic phytoplankton (Collins and Bell 2004; Lohbeck et al. 2012; Perrineau et al. 2014). Very few beneficial mutations are expected to be fixed within 300 generations in *Escherichia coli* (Barrick et al. 2009), suggesting that the changes in fitness in our experiments may be due to changes in population genetic structure or epigenetic mechanisms such as gene methylation. But in the diatom *Thalassiosira pseudonana*, over 225,000 mutations were detected, 7000 fixed, over 300 generations (Schaum et al. 2018). A transcriptomic analysis of two closely related temperate diatom species with different optimal growth temperatures indicates that changes in baseline gene expression can influence differences in optimal growth temperature and temperature performance curves (Liang et al. 2019). The fitness trajectories we observed are consistent with the accumulation of many changes of small effect. By contrast,

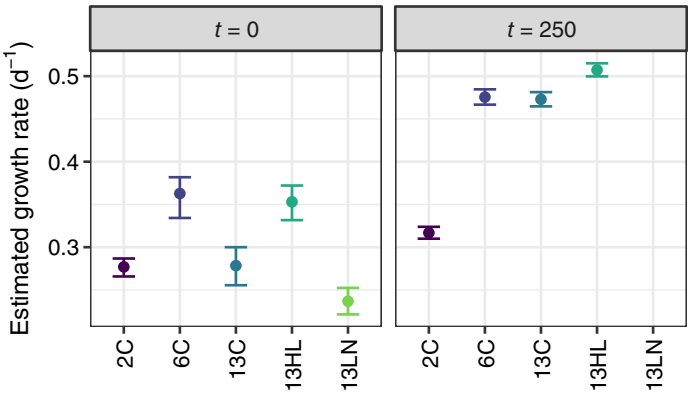

Fig. 2. Estimated exponential growth rates (d^{-1}) at the initiation (t = 0) and after 250 generations of exposure (t = 250). The horizontal axis indicates the experimental treatment according to the following legend: 2°C (2C), 6°C (6C), 13°C (13C), 13°C and high irradiance (13HL), and 13°C and periodic nitrate limitation (13LN). Note that 13LN lines were terminated at 170 generations and therefore are not shown on the second panel. An alternative presentation (Supporting Information Fig. S1) emphasizes the change in exponential growth rates within treatments over time.

a few changes with large effects on fitness would likely lead to distinct fitness trajectories for each culture lineage within a treatment and jump discontinuities in growth rate over time. On longer timescales of thousands of generations, *de novo* mutations and large changes in fitness may become important (Barrick et al. 2009).

Novel conditions present a new selection regime, creating opportunities for large and rapid changes in fitness through selection. Initially the strains will be relatively maladapted to the new conditions, although some changes in conditions may be too severe to permit survival and subsequent adaptation. *M. polaris* was isolated from the North Water Polynya (76°N) and would have frequently encountered temperatures between 2°C and 6°C in the environment, but would have rarely experienced temperatures above 10°C (Lovejoy et al. 2007). Accordingly, the linear rate of change and ultimate maximum fitness change were largest in the 13°C relative to the 2°C and 6°C treatments. Our 13°C high light and repeated low nitrate treatments presented two more evolutionary challenges to *M. polaris* to test its evolutionary potential in response to additional environmental conditions in addition to temperature. Early physiological work on this strain showed highest growth rates under low light conditions (< 50 μmol m^{-2} s^{-1}) (Lovejoy et al. 2007). In this experiment, an increase in irradiance from 100 to 220 μmol m^{-2} s^{-1} led to an immediate increase (within 10 generations) in growth rate at 13°C, restoring growth rate to the initial maximum growth rate achieved at 6°C and 100 μmol m^{-2} s^{-1} (Fig. 1), followed by gradual increases in growth rate essentially identical to those observed in the 13C treatment (Table 1). The periodic low nitrate stress treatment resulted in the largest and most rapid increase in exponential growth rate of all the treatments over the subsequent 160 generations. This change may be a result of an increase in the maximum growth rate during exponential phase or a change in duration of the lag or stationary phases or a change in resource use efficiency. We hypothesize that *M. polaris* may have adapted to the repeated periodic low nitrate treatment through a reduction in lag phase duration, increase in high affinity uptake, or by increase in resource use efficiency. In *E. coli*, increases of growth rate have been associated with large decreases in lag phase over less than 100 generations (Oxman et al. 2008). Potential evolutionary responses to higher light and periodic nutrient depletion at the cooler treatments (2°C and 6°C) and the potential for interaction between these treatments at all temperatures requires further investigation. In summary, treatments that are less representative of typical ancestral conditions result in larger relative increases in fitness through selection unless constrained by genetic and biophysical challenges to improving fitness.

Climate change is anticipated to lead to widespread warming throughout the surface ocean. A survey of maximum growth rates across phytoplankton under ideal conditions reveals a linear to exponential increase in maximum growth rate with increasing temperature up to a threshold temperature followed by rapid declines in growth rates at even higher temperature (Eppley 1972; Montagnes et al. 2003; Kremer et al. 2017). Each individual species has its own characteristic temperature for maximum growth rate and critical temperature at which growth ceases. In the absence of adaptation to changing temperatures, many cold-adapted Arctic species such as *M. polaris* CCMP 2099 may eventually exhibit decreases in growth rate with climate warming. Alternatively, the cross-species pattern in maximum growth rate may define a potential evolutionary increase in growth rates with increasing temperature.

Metabolic rates, including growth rate μ, are commonly modeled as varying with temperature according to an Arrhenius function,

$$\mu = \mu_0 \exp\left(\frac{E_a}{k}\left(\frac{1}{T_0} - \frac{1}{T}\right)\right) \quad (3)$$

where μ_0 is the growth rate at the reference temperature T_0, $k = 8.62 \times 10^{-5}$ eV K^{-1} is Boltzmann's constant, E_a = 0.32–0.65- eV is an estimated activation energy for biochemical reactions in a cell (López-Urrutia et al. 2006), and T is temperature in Kelvin. The ratio μ/μ_0 described by the Arrhenius function is similar in effect to the commonly used Q_{10}-law: $\mu_2/\mu_1 = Q_{10}^{(T2 - T1)/10}$. As with the activation energy, Q_{10} is empirically determined and has been estimated to be in the range of 1.53–1.88 for phytoplankton (Eppley 1972; Montagnes et al. 2003) and for other organisms in the range 2–3. Cross-species maximum growth rates appear to vary with temperature according to this relationship and thus it can be used to define a hypothesis for the maximum growth rates attainable in an

evolutionary experiment. Using E_a = 0.40 eV, we project that *Micromonas* could achieve a maximum growth rate at 13°C which is 50% higher than initially observed at 6°C. In our experiment, the evolutionary outcome in the 13°C treatment was a growth rate of 0.47 d^{-1} after 250 generations and we project an ultimate maximum growth rate of 0.57 d^{-1} ($\mu_0 + \mu_D$ = 0.28 + 0.29 d^{-1}, Table 1) which is 58% larger than the initial maximum growth rate at the optimal temperature of 6°C, in accordance with our projection. The projected increase in the 13°C high-light treatment was essentially the same, although the growth rates achieved were larger due to the adaptation to elevated irradiance. The growth rate in the 13°C periodically low-nitrate treatment increased linearly and our experiment did not yield a convincing estimate of its anticipated maximum growth rate. Modest projected increases in growth rate were observed for both the 2°C and 6°C lines of 0.07 d^{-1} and 0.18 d^{-1}, respectively, which we interpret as adaptation to the specific culture conditions rather than adaptations to temperature treatment as this species was isolated from an environment where these temperatures were commonly encountered.

Our results suggest that potential evolutionary increases in growth rate within a species to a temperature change may be determined by mechanisms that link temperature to maximum growth rate across species over a wide range of temperatures (Eppley 1972; Kremer et al. 2017). Extrapolating from our results, phytoplankton may have the evolutionary potential to adapt to increases in temperature anticipated due to climate change over the coming century by overcoming the damaging effects of elevated temperature and increasing their maximum growth rate. Although we have tested the combined effects of temperature increase and increased irradiance or periodic nitrate limitation, the ultimate consequences of climate change will be more nuanced than the simple treatments explored here. Other priorities for future research include evaluating how multiple environmental conditions and biotic factors, including viruses (Piedade et al. 2018), phagotrophic ability (Mckie-Krisberg and Sanders 2014), and trade-offs between photosynthetic and respiratory processes (Padfield et al. 2016; Barton et al. 2018), may influence the evolutionary capacity of *Micromonas* to respond to climate change.

References

Ardyna, M., M. Babin, E. Devred, A. Forest, M. Gosselin, P. Raimbault, and J.-É. Tremblay. 2017. Shelf-basin gradients shape ecological phytoplankton niches and community composition in the coastal Arctic Ocean (Beaufort Sea). Limnol. Oceanogr. **62**: 2113–2132. doi:10.1002/lno.10554

Arrigo, K., and G. L. Van Dijken. 2011. Secular trends in Arctic Ocean net primary production. J. Geophys. Res. **116**: 1–15. doi:10.1029/2011JC007151

Balzano, S., P. Gourvil, R. Siano, M. Chanoine, D. Marie, S. Lessard, D. Sarno, and D. Vaulot. 2012. Diversity of cultured photosynthetic flagellates in the northeast Pacific and Arctic Oceans in summer. Biogeosciences **9**: 4553–4571. doi:10.5194/bg-9-4553-2012

Barrick, J. E., D. S. Yu, S. H. Yoon, H. Jeong, T. K. Oh, D. Schneider, R. E. Lenski, and J. F. Kim. 2009. Genome evolution and adaptation in a long-term experiment with *Escherichia coli*. Nature **461**: 1243–1247. doi:10.1038/nature08480

Barton, S., J. Jenkins, A. Buckling, C. E. Schaum, N. Smirnoff, and G. Yvon-Durocher. 2018. Universal metabolic constraints on the thermal tolerance of marine phytoplankton. bioRxiv: 10.1101/358002. doi:10.1101/358002

Bélanger, S., M. Babin, and J. É. Tremblay. 2013. Increasing cloudiness in Arctic damps the increase in phytoplankton primary production due to sea ice receding. Biogeosciences **10**: 4087–4101. doi:10.5194/bg-10-4087-2013

Bell, G., and S. Collins. 2008. Adaptation, extinction and global change. Evol. Appl. **1**: 3–16. doi:10.1111/j.1752-4571.2007.00011.x

Bürkner, P.-C. 2018. Advanced Bayesian multilevel modeling with the R package brms. R J. **10**: 395–411. doi:10.32614/RJ-2018-017

Capotondi, A., M. A. Alexander, N. A. Bond, E. N. Curchitser, and J. D. Scott. 2012. Enhanced upper ocean stratification with climate change in the CMIP3 models. J. Geophys. Res. **117**: C04031. doi:10.1029/2011JC007409

Carpenter, B., A. Gelman, M. D. Hoffman, D. Lee, B. Goodrich, M. Betancourt, and A. Riddell. 2017. Stan: A probabilistic programming language. J. Stat. Softw. 76. doi:10.18637/jss.v076.i01

Coella-Camba, A., and S. Agusti. 2017. Thermal thresholds of phytoplankton growth in polar waters and their consequences for a warming polar ocean. Front. Mar. Sci. **4**: 1–1222. doi:10.3389/fmars.2017.00168

Collins, S., and G. Bell. 2004. Phenotypic consequences of 1000 generations of selection at elevated CO_2 in a green alga. Nature **431**: 566–569. doi:10.1038/nature02945

Demory, D., and others. 2019. Picoeukaryotes of the *Micromonas* genus: Sentinels of a warming ocean. ISME J. **13**: 132–146. doi:10.1038/s41396-018-0248-0

Eppley, R. W. 1972. Temperature and phytoplankton growth in the sea. Fish. Bull. **70**: 1063–1085.

Finkel, Z. V., J. Beardall, K. J. Flynn, A. Quigg, T. A. V. Rees, and J. A. Raven. 2010. Phytoplankton in a changing world: Cell size and elemental stoichiometry. J. Plankton Res. **32**: 119–137. doi:10.1093/plankt/fbp098

Hoppe, C. J. M., C. M. Flintrop, and B. Rost. 2018. The Arctic picoeukaryote *Micromonas pusilla* benefits synergistically from warming and ocean acidification. Biogeosciences **15**: 4353–4365. doi:10.5194/bg-15-4353-2018

Kremer, C. T., M. K. Thomas, and E. Litchman. 2017. Temperature- and size-scaling of phytoplankton population

growth rates: Reconciling the Eppley curve and the metabolic theory of ecology. Limnol. Oceanogr. **62**: 1658–1670. doi:10.1002/lno.10523

Laws, E. A., P. G. Falkowski, W. O. J. Smith, H. Ducklow, and J. J. Mccarthy. 2000. Temperature effects on export production in the open ocean. Global Biogeochem. Cycles **14**: 1231–1246. doi:10.1029/1999GB001229

Li, W. K. W., F. A. Mclaughlin, C. Lovejoy, and E. C. Carmack. 2009. Smallest algae thrive as the Arctic Ocean freshens. Science **326**: 539. doi:10.1126/science.1179798

Liang, Y., J. A. Koester, J. D. Liefer, A. J. Irwin, and Z. V. Finkel. 2019. Molecular mechanisms of temperature acclimation and adaptation in marine diatoms. ISME J. **13**: 2415–2425. doi:10.1038/s41396-019-0441-9

Lohbeck, K. T., U. Riebesell, S. Collins, and T. B. H. Reusch. 2012. Functional genetic divergence in high CO_2 adapted *Emiliania huxleyi* populations. Evolution **67**: 1892–1900. doi:10.1111/j.1558-5646.2012.01812.x

López-Urrutia, A., E. San Martin, R. P. Harris, and X. Irigoien. 2006. Scaling the metabolic balance of the oceans. Proc. Natl. Acad. Sci. USA **103**: 8739–8744. doi:10.1073/pnas.0601137103

Lovejoy, C., and others. 2007. Distribution, phylogeny, and growth of cold-adapted picoprasinophytes in Arctic Seas. J. Phycol. **43**: 78–89. doi:10.1111/j.1529-8817.2006.00310.x

Maechler, M., and others. 2018. robustbase: Basic robust statistics R package version 0.93–3. R package.

Mckie-Krisberg, Z. M., and R. W. Sanders. 2014. Phagotrophy by the picoeukaryotic green alga *Micromonas*: Implications for Arctic Oceans. ISME J. **8**: 2151. doi:10.1038/ismej.2014.126

Montagnes, D. J. S., S. A. Kimmance, and D. Atkinson. 2003. Using Q_{10}: Can growth rates increase linearly with temperature? Aquat. Microb. Ecol. **32**: 307–313. doi:10.3354/ame032307

Not, F., and others. 2005. Late summer community composition and abundance of photosynthetic picoeukaryotes in Norwegian and Barents Seas. Limnol. Oceanogr. **50**: 1677–1686. doi:10.4319/lo.2005.50.5.1677

Osborne, E., J. Richter-Menge, and M. Jeffries [eds.]. 2018. Arctic report card 2018. NOAA Arctic Program. https://www.arctic.noaa.gov/Report-Card

Oxman, E., U. Alon, and E. Dekel. 2008. Defined order of evolutionary adaptations: Experimental evidence. Evolution **62**: 1547–1554. doi:10.1111/j.1558-5646.2008.00397.x

Padfield, D., G. Yvon-Durocher, A. Buckling, S. Jennings, and G. Yvon-Durocher. 2016. Rapid evolution of metabolic traits explains thermal adaptation in phytoplankton. Ecol. Lett. **19**: 133–142. doi:10.1111/ele.12545

Perrineau, M.-M., J. Gross, E. Zelzion, D. C. Price, O. Levitan, J. Boyd, and D. Bahattacharya. 2014. Using natural selection to explore the adaptive potential of *Chlamydomonas reinhardtii*. PLoS One **9**: e92533. doi:10.1371/journal.pone.0092533

Piedade, G. J., E. M. Wesdorp, E. Montenegro-Borbolla, D. S. Maat, and C. P. D. Brussaard. 2018. Influence of irradiance and temperature on the virus MpoV-45T infecting the Arctic picophytoplankter *Micromonas polaris*. Viruses **10**: 676. doi:10.3390/v10120676

Schaum, C. E., B. Rost, and S. Collins. 2016. Environmental stability affects phenotypic evolution in a globally distributed marine picoplankton. ISME J. **10**: 75–84. doi:10.1038/ismej.2015.102

Schaum, C.-E., A. Bucking, N. Smirnoff, D. J. Studholme, and G. Yvon-Durocher. 2018. Environmental fluctuations accelerate molecular evolution of thermal tolerance in a marine diatom. Nat. Commun. **9**: 1719. doi:10.1038/s41467-018-03906-5

Simon, N., and others. 2017. Revision of the genus *Micromonas* Manton et Parke (Chlorophyta, Mamiellophyceae), of the type species *M. pusilla* (butcher) Manton & Parke and of the species *M. commoda* van Baren, Bachy and Worden and description of two new species based on the genetic and phenotypic characterization of cultured isolates. Protist **168**: 612–635. doi:10.1016/j.protis.2017.09.002

Tremblay, J. É., L. G. Anderson, P. Matrai, S. Bélanger, C. Michel, P. Coupel, and M. Reigstad. 2015. Global and regional drivers of nutrient supply, primary production and CO_2 drawdown in the changing Arctic Ocean. Prog. Oceanogr. **139**: 171–196. doi:10.1016/j.pocean.2015.08.009

Vancoppenolle, M., L. Bopp, G. Madec, J. Dunne, T. Ilyina, P. R. Halloran, and N. Steiner. 2013. Future Arctic Ocean primary productivity from CMIP5 simulations: Uncertain outcome, but consistent mechanisms. Global Biogeochem. Cycles **27**: 605–619. doi:10.1002/gbc.20055

Walworth, N. G., M. D. Lee, F.-X. Fu, D. A. Hutchins, and E. A. Webb. 2016. Molecular and physiological evidence of genetic assimilation to high CO_2 in the marine nitrogen fixer *Trichodesmium*. Proc. Natl. Acad. Sci. USA **113**: E7367–E7374. doi:10.1073/pnas.1605202113

Acknowledgments

We were supported by NSERC Canada (A.J.I., Z.V.F.) and the CRC program (Z.V.F.).

Submitted 21 March 2019
Revised 08 November 2019
Accepted 12 November 2019